Robust Adaptive Beamforming Using Worst-Case Performance Optimization: A Solution to the Signal Mismatch Problem

Sergiy A. Vorobyov, *Member, IEEE*, Alex B. Gershman, *Senior Member, IEEE*, and Zhi-Quan Luo, *Member, IEEE*

Abstract—Adaptive beamforming methods are known to degrade if some of underlying assumptions on the environment, sources, or sensor array become violated. In particular, if the desired signal is present in training snapshots, the adaptive array performance may be quite sensitive even to slight mismatches between the presumed and actual signal steering vectors (spatial signatures). Such mismatches can occur as a result of environmental nonstationarities, look direction errors, imperfect array calibration, distorted antenna shape, as well as distortions caused by medium inhomogeneities, near–far mismatch, source spreading, and local scattering. The similar type of performance degradation can occur when the signal steering vector is known exactly but the training sample size is small.

In this paper, we develop a new approach to robust adaptive beamforming in the presence of an arbitrary unknown signal steering vector mismatch. Our approach is based on the optimization of worst-case performance. It turns out that the natural formulation of this adaptive beamforming problem involves minimization of a quadratic function subject to infinitely many nonconvex quadratic constraints. We show that this (originally intractable) problem can be reformulated in a convex form as the so-called second-order cone (SOC) program and solved efficiently (in polynomial time) using the well-established interior point method. It is also shown that the proposed technique can be interpreted in terms of diagonal loading where the optimal value of the diagonal loading factor is computed based on the known level of uncertainty of the signal steering vector. Computer simulations with several frequently encountered types of signal steering vector mismatches show better performance of our robust beamformer as compared with existing adaptive beamforming algorithms.

Index Terms—Optimal diagonal loading, robust adaptive beamforming, second-order cone programming, signal mismatch problem, worst-case performance optimization.

I. INTRODUCTION

IN recent decades, adaptive beamforming has been widely used in wireless communications, microphone array speech processing, radar, sonar, medical imaging, radio astronomy, and other areas. A traditional approach to the design of adaptive beamformers assumes that the desired signal components are not present in training data [1]. In this case, several rapidly converging techniques have been developed [1]–[5] that are applicable to problems with small training sample size. Although the assumption of signal-free training snapshots may be true in some areas (such as radar), there are numerous applications where the observations are always "contaminated" by the signal component. Such applications, for example, include mobile communications, passive source location, microphone array speech processing, medical imaging, and radio astronomy. It is well known that even in the ideal case where the signal steering vector is exactly known, the presence of the signal of interest in training data cell may dramatically reduce the convergence rates of adaptive beamforming algorithms as compared with the signal-free training data case [6]. This may cause a substantial degradation of the performance of adaptive beamforming techniques in situations of small training sample size.

When adaptive arrays are applied to practical problems, the performance degradation of adaptive beamforming techniques may become even more pronounced than in the aforementioned ideal case because some of underlying assumptions on the environment, sources, or sensor array can be violated and this may cause a mismatch between the nominal (presumed) and actual signal steering vectors. Adaptive array techniques are known to be very sensitive even to slight mismatches of such type that can easily occur in practical situations as a consequence of look direction and signal pointing errors [7], [8] or imperfect array calibration and distorted antenna shape [9]. Other common causes of model mismatch include array manifold mismodeling due to source wavefront distortions resulting from environmental inhomogeneities [10], [11], near–far problem [12], source spreading and local scattering [13]–[16], as well as other effects [17]. In such cases, robust approaches to adaptive beamforming are required [17]–[19].

There are several existing approaches to robust adaptive beamforming. The most common is the so-called linearly constrained minimum variance (LCMV) beamformer, which provides robustness against uncertainty in the signal look direction. Recently, several other techniques addressing this type of mismatch have been developed (see [19] and references therein). However, the applicability of these techniques is limited by scenarios with look direction mismatches only. If any other types of steering vector mismatch become dominant (e.g., mismatches due to array perturbations, array manifold mismodeling, wavefront distortions, or source local scattering), these methods cannot be expected to provide sufficient robustness improvements [17].

Several other approaches are known to be able to partly overcome the problem of arbitrary steering vector mismatches. The most popular of them are the quadratically constrained beamformer (whose implementation is based on the so-called *diagonal loading* of the sample covariance matrix [4], [18], [20]) and the eigenspace-based beamformer [6], [21]. However, the main shortcoming of the former approach is that it is not clear how to obtain the optimal value of the diagonal loading factor based on the known level of uncertainty of the signal steering vector, whereas the latter approach is essentially ineffective at low signal-to-noise ratios (SNRs) and when the dimension of the signal-plus-interference subspace is high.[1] This, unfortunately, makes it difficult to apply the eigenspace-based beamformer to wireless communications where the dimension of the signal-plus-interference subspace may be uncertain and relatively high due to the effects of signal local scattering [13]–[16].

In this paper (also see [22]–[24]), we develop a new powerful approach to robust adaptive beamforming in the presence of an arbitrary unknown steering vector mismatch. Our approach is based on the optimization of worst-case performance. It turns out that the natural formulation of this problem involves minimization of a quadratic function subject to infinitely many nonconvex quadratic constraints and therefore is NP-hard[2] to solve. However, we show that this robust adaptive beamforming problem can be reformulated as a convex second-order cone (SOC) program and solved efficiently (in polynomial time) via the well-established interior point method (see [27]–[29]). This result is somewhat surprising from the optimization theory standpoint and is based on a procedure that transforms a semi-infinite nonconvex quadratically constrained homogeneous quadratic minimization problem to a convex SOC program. We show that our beamformer can be interpreted as a diagonal loading approach[3] in which the optimal value of the diagonal loading factor is computed based on the known upper bound on the norm of the signal steering vector mismatch.

Computer simulations with several frequently encountered types of signal steering vector mismatches show a visible performance gain of the proposed beamformer over other traditional and robust adaptive beamforming techniques.

Our paper is organized as follows. Some background of adaptive beamforming is presented in Section II, where several popular robust adaptive beamforming techniques are overviewed. In Section III, we first describe a new formulation of robust adaptive beamforming based on the optimization of worst-case performance. Then, we establish the diagonal loading based interpretation of our robust adaptive beamforming problem and convert it to a convex SOC problem that can be efficiently solved using the well-established interior point algorithms. Section IV presents our simulation results where the performance of the proposed method is compared with the existing algorithms in situations with different types of the signal steering vector mismatch. Section V contains our concluding remarks.

---

[1]Additionally, this dimension must be exactly known in this technique.

[2]In optimization theory, NP-hard problems represent a class of extremely difficult problems that have no known polynomial-time solutions [25].

[3]Very recently, another robust worst-case optimization-based beamformer (which also belongs to the class of diagonal loading techniques) has been independently formulated; see [26].

II. BACKGROUND

The output of a narrowband beamformer is given by

$$y(k) = \boldsymbol{w}^H \boldsymbol{x}(k)$$

where k is the time index, $\boldsymbol{x}(k) = [x_1(k),\ldots,x_M(k)]^T \in \mathcal{C}^{M\times 1}$ is the complex vector of array observations, $\boldsymbol{w} = [w_1,\ldots,w_M]^T \in \mathcal{C}^{M\times 1}$ is the complex vector of beamformer weights, M is the number of array sensors, and $(\cdot)^T$ and $(\cdot)^H$ stand for the transpose and Hermitian transpose, respectively. The observation (training snapshot) vector is given by

$$\begin{aligned} \boldsymbol{x}(k) &= \boldsymbol{s}(k) + \boldsymbol{i}(k) + \boldsymbol{n}(k) \\ &= s(k)\boldsymbol{a} + \boldsymbol{i}(k) + \boldsymbol{n}(k) \end{aligned} \quad (1)$$

where $\boldsymbol{s}(k)$, $\boldsymbol{i}(k)$, and $\boldsymbol{n}(k)$ are the desired signal, interference, and noise components, respectively. Here, $s(k)$ is the signal waveform, and $\boldsymbol{a}$ is the signal steering vector. The weight vector can be found from the maximum of the signal-to-interference-plus-noise ratio (SINR) [5]

$$\mathrm{SINR} = \frac{\sigma_s^2 |\boldsymbol{w}^H \boldsymbol{a}|^2}{\boldsymbol{w}^H \boldsymbol{R}_{i+n} \boldsymbol{w}} \quad (2)$$

where

$$\boldsymbol{R}_{i+n} = E\left\{ (\boldsymbol{i}(k) + \boldsymbol{n}(k))(\boldsymbol{i}(k) + \boldsymbol{n}(k))^H \right\} \quad (3)$$

is the $M \times M$ interference-plus-noise covariance matrix, and σ_s^2 is the signal power. It is easy to find the solution for the weight vector by maintaining a distortionless response toward the desired signal and minimizing the output interference-plus-noise power [5]. Hence, the maximization of (2) is equivalent to [5]

$$\min_{\boldsymbol{w}} \boldsymbol{w}^H \boldsymbol{R}_{i+n} \boldsymbol{w} \qquad \text{subject to} \qquad \boldsymbol{w}^H \boldsymbol{a} = 1. \quad (4)$$

From (4), the following well-known solution can be found for the optimal weight vector [5]:

$$\boldsymbol{w}_{\mathrm{opt}} = \alpha \boldsymbol{R}_{i+n}^{-1} \boldsymbol{a} \quad (5)$$

where $\alpha = \left(\boldsymbol{a}^H \boldsymbol{R}_{i+n}^{-1} \boldsymbol{a} \right)^{-1}$ is the normalization constant that does not affect the output SINR (2) and, therefore, will be omitted in the interest of brevity. The solution (5) is commonly referred to as the minimum variance distortionless response (MVDR) beamformer [5], [30].

In practical applications, the exact interference-plus-noise covariance matrix $\boldsymbol{R}_{i+n}$ is unavailable. Therefore, the sample covariance matrix

$$\hat{\boldsymbol{R}} = \frac{1}{N} \sum_{n=1}^{N} \boldsymbol{x}(n)\boldsymbol{x}^H(n) \quad (6)$$

is used instead of (3) (see [1]). Here, N is the number of training snapshots (also termed the *training sample size*). In this case, (4) should be rewritten as

$$\min_{\boldsymbol{w}} \boldsymbol{w}^H \hat{\boldsymbol{R}} \boldsymbol{w} \qquad \text{subject to} \qquad \boldsymbol{w}^H \boldsymbol{a} = 1. \quad (7)$$

The solution to this problem is commonly referred to as the sample matrix inversion (SMI) algorithm, whose weight vector (after omitting the immaterial constant $\alpha = 1/\boldsymbol{a}^H \hat{\boldsymbol{R}}^{-1} \boldsymbol{a}$) is given by [1]

$$\boldsymbol{w}_{\text{SMI}} = \hat{\boldsymbol{R}}^{-1} \boldsymbol{a}. \tag{8}$$

When the signal component is present in the training data cell (cf. (1)), the use of the sample covariance matrix (6) in place of the true interference-plus-noise covariance matrix (3) affects the performance of the SMI algorithm dramatically [6]. It is well known since the classic paper [1] that in the case of signal-free training samples, the use of weight vector (8) provides rapid convergence of the output SINR to its optimal value

$$\text{SINR}_{\text{opt}} = \sigma_s^2 \boldsymbol{a}^H R_{i+n}^{-1} \boldsymbol{a} \tag{9}$$

so that the average performance losses relative to (9) are less than 3 dB if $N \geq 2M$. However, this is no longer true if the training snapshots are "contaminated" by the signal component. It was shown in [6] that in the latter case the convergence to (9) becomes much slower and generally requires $N \gg M$.

Another essential shortcoming of the SMI algorithm is that it does not provide sufficient robustness against a mismatch between the presumed and actual signal steering vectors $\boldsymbol{a}$ and $\tilde{\boldsymbol{a}}$. Here, $\tilde{\boldsymbol{a}}$ denotes the actual steering vector that characterizes the spatial signature of the signal. In the mismatched case

$$\tilde{\boldsymbol{a}} = \boldsymbol{a} + \boldsymbol{\Delta} \neq \boldsymbol{a} \tag{10}$$

where $\boldsymbol{\Delta}$ is an unknown complex vector that describes the effect of steering vector distortions. As a result, the SMI beamformer tends to "interpret" the signal components in array observations as an interference and tries to suppress these components by means of adaptive nulling instead of maintaining distortionless response toward $\tilde{\boldsymbol{a}}$ (see [6] and [17]).

In the mismatched case, (2) and (9) should be rewritten as

$$\text{SINR} = \frac{\sigma_s^2 \left| \boldsymbol{w}^H \tilde{\boldsymbol{a}} \right|^2}{\boldsymbol{w}^H R_{i+n} \boldsymbol{w}} \tag{11}$$

and

$$\text{SINR}_{\text{opt}} = \sigma_s^2 \tilde{\boldsymbol{a}}^H R_{i+n}^{-1} \tilde{\boldsymbol{a}} \tag{12}$$

respectively. Several robust modifications of the SMI algorithm have been developed to improve its performance in the above-mentioned cases with signal steering vector mismatches and small training sample size. One of the most popular robust approaches is the so-called loaded SMI (LSMI) algorithm, which is based on the diagonal loading of the sample covariance matrix [4], [18]. The essence of this approach is to replace the conventional sample covariance matrix $\hat{\boldsymbol{R}}$ by the so-called diagonally loaded covariance matrix

$$\hat{R}_{\text{dl}} = \xi I + \hat{R} \tag{13}$$

in the SMI algorithm (8). Here, ξ is a diagonal loading factor, and $\boldsymbol{I}$ is the identity matrix. Using (13), we can write the LSMI weight vector in the following form [4]:

$$\boldsymbol{w}_{\text{LSMI}} = \hat{R}_{\text{dl}}^{-1} \boldsymbol{a} = (\xi I + \hat{R})^{-1} \boldsymbol{a}. \tag{14}$$

The main problem of the LSMI method is how to chose the diagonal loading factor ξ. Cox *et al.* [18] proposed to use the so-called *white noise gain constraint* to obtain reasonable values of this parameter. Unfortunately, it is not clear how to relate the parameters of the white noise gain constraint and the level of uncertainty of the signal steering vector. Furthermore, the relationship between the diagonal loading factor and the parameters of the white noise gain constraint is not simple, and to satisfy this constraint, a multistep iterative procedure is required to adjust the diagonal loading factor [18]. Each step of this iterative procedure involves an update of the inverse of the diagonally loaded covariance matrix, and as a result, the total computational complexity of adaptive beamforming with the white noise gain constraint may be higher than that of the SMI algorithm. Because of this, the diagonal loading factor is usually chosen in a more *ad hoc* way, typically about $10\sigma^2$, where σ^2 is the noise power in a single sensor.

Another popular approach to robust adaptive beamforming in the general case of an arbitrary mismatch is the so-called eigenspace-based beamformer [6], [21] whose key idea is to use, instead of the presumed steering vector $\boldsymbol{a}$, the projection of $\boldsymbol{a}$ onto the sample signal-plus-interference subspace. The eigen-decomposition of (6) yields

$$\hat{\boldsymbol{R}} = \boldsymbol{E}\boldsymbol{\Lambda}\boldsymbol{E}^H + \boldsymbol{G}\boldsymbol{\Gamma}\boldsymbol{G}^H$$

where the matrix $\boldsymbol{E} \in \mathcal{C}^{M \times (J+1)}$ contains the $J+1$ signal-plus-interference subspace eigenvectors of $\hat{\boldsymbol{R}}$, and the diagonal matrix $\boldsymbol{\Lambda} \in \mathcal{C}^{(J+1) \times (J+1)}$ contains the corresponding eigenvalues of $\hat{\boldsymbol{R}}$. Similarly, the matrix $\boldsymbol{G} \in \mathcal{C}^{M \times (M-J-1)}$ contains the $M - J - 1$ noise-subspace eigenvectors of $\hat{\boldsymbol{R}}$, whereas the diagonal matrix $\boldsymbol{\Gamma} \in \mathcal{C}^{(M-J-1) \times (M-J-1)}$ is built from the corresponding eigenvalues. Here, J is the number of interfering sources (or, mathematically, the rank of the interference subspace), which is assumed to be known. The weight vector of the eigenspace-based beamformer is given by

$$\boldsymbol{w}_{\text{eig}} = \hat{\boldsymbol{R}}^{-1} \boldsymbol{v} \tag{15}$$

where

$$\boldsymbol{v} = \boldsymbol{P}_E \boldsymbol{a}, \qquad \boldsymbol{P}_E = \boldsymbol{E}\boldsymbol{E}^H \tag{16}$$

are the projected steering vector and the orthogonal projection matrix onto the signal-plus-interference subspace, respectively. Inserting (16) into (15), the latter equation can be rewritten as

$$\boldsymbol{w}_{\text{eig}} = \boldsymbol{E}\boldsymbol{\Lambda}^{-1}\boldsymbol{E}^H \boldsymbol{a}. \tag{17}$$

The eigenspace-based beamformer is known to be one of the most powerful robust techniques applicable to arbitrary steering vector mismatch case [21]. However, an essential shortcoming of this approach is that it is limited to high SNR cases because at low SNR the estimation of the projection matrix onto the signal-plus-interference subspace breaks down because of a high probability of subspace swaps [31], [32]. Moreover, the eigenspace-based beamformer is efficient only if the dimension of the signal-plus-interference subspace is low and known exactly. This makes it difficult to apply the eigenspace-based beamformer to wireless communications where the dimension

of the signal-plus-interference subspace may be uncertain and relatively high due to the effects of source scattering [13]–[16].

III. NEW APPROACH TO ROBUST BEAMFORMING

In this section, we develop a new adaptive beamformer that is robust against an arbitrary signal steering vector mismatch and small training sample size. Our approach is based on the worst-case performance optimization. We begin with the formulation of the robust adaptive beamforming problem and then develop a convex optimization-based implementation of our adaptive beamformer using SOC programming.

A. Formulation

We assume that in practical applications, the norm of the steering vector distortion $\mathbf{\Delta}$ can be bounded[4] [33] by some known constant $\varepsilon > 0$:

$$\|\mathbf{\Delta}\| \leq \varepsilon. \tag{18}$$

Then, the actual signal steering vector belongs to the set

$$\mathcal{A}(\varepsilon) \triangleq \{\mathbf{c} \,|\, \mathbf{c} = \mathbf{a} + \mathbf{e}, \ \|\mathbf{e}\| \leq \varepsilon\}. \tag{19}$$

Indeed, if $\mathbf{e} = \mathbf{\Delta}$, then, according to (10), $\mathbf{c} = \tilde{\mathbf{a}}$. Since $\tilde{\mathbf{a}}$ can be any vector in (19), we impose a constraint that for all vectors that belong to $\mathcal{A}(\varepsilon)$, the absolute value[5] of the array response should not be smaller than one, i.e.,

$$|\mathbf{w}^H \mathbf{c}| \geq 1 \qquad \text{for all} \qquad \mathbf{c} \in \mathcal{A}(\varepsilon). \tag{20}$$

Using (20), the robust formulation of adaptive beamformer can be written as the following constrained minimization problem:

$$\min_{\mathbf{w}} \mathbf{w}^H \hat{R} \mathbf{w} \text{ subject to } |\mathbf{w}^H \mathbf{c}| \geq 1 \text{ for all } \mathbf{c} \in \mathcal{A}(\varepsilon). \tag{21}$$

Note that (21) represents a modified version of (7). The main modification of (7) is that instead of requiring fixed distortionless response toward the single steering vector $\mathbf{a}$, in (21), such distortionless response is maintained by means of inequality constraints[6] for a continuum of all possible steering vectors given by the set $\mathcal{A}(\varepsilon)$. Hence, the constraints in (21) guarantee that the distortionless response will be maintained in the *worst case*, i.e., for the particular vector $\mathbf{c}$ that corresponds to the smallest value of $|\mathbf{w}^H \mathbf{c}|$. Therefore, such a design should improve the beamformer robustness against signal steering vector mismatches that satisfy (18) because in this case, the mismatched vector $\tilde{\mathbf{a}}$ belongs to the set $\mathcal{A}(\varepsilon)$.

For each choice of $\mathbf{c} \in \mathcal{A}(\varepsilon)$, the condition $|\mathbf{w}^H \mathbf{c}| \geq 1$ represents a nonlinear and *nonconvex* constraint on $\mathbf{w}$. Since there is an infinite number of vectors $\mathbf{c}$ in $\mathcal{A}(\varepsilon)$, there is an infinite number of such constraints. Hence, (21) is a semi-infinite

---

[4]Note that this corresponds to a much more general class of mismatches than considered in [34], where the bounds on the mismatch vector itself are used rather than that on the norm of this vector.

[5]An important issue that is beyond our present consideration is how to control the phase of the beam response. This issue may be critical when, for example, adaptive beamforming has to be performed over frequency subbands whose outputs must be coherently integrated.

[6]Constraints in the form of inequality (sometimes referred to as *soft constraints*) are used in other adaptive beamforming techniques as well [35]–[37].

nonconvex quadratic program. It is well known that the general nonconvex quadratically constrained quadratic programming problem is NP-hard and, thus, intractable. However, as we will show next, due to the special structure of the objective function and the constraints, the problem (21) can be reformulated, surprisingly, as a convex SOC program and, thus, solved efficiently (in polynomial time) via the well established interior point method.

Let us first convert the semi-infinite nonconvex constraints to a single constraint that corresponds to the worst-case constraint from (20). In particular, (21) can be equivalently described as

$$\min_{\mathbf{w}} \mathbf{w}^H \hat{R} \mathbf{w} \quad \text{subject to} \quad \min_{\mathbf{c} \in \mathcal{A}(\varepsilon)} |\mathbf{w}^H \mathbf{c}| \geq 1. \tag{22}$$

According to (19), we can rewrite the constraint of (22) as

$$\min_{\mathbf{e} \in \mathcal{D}(\varepsilon)} |\mathbf{w}^H \mathbf{a} + \mathbf{w}^H \mathbf{e}| \geq 1$$

where the set $\mathcal{D}(\varepsilon)$ is defined as

$$\mathcal{D}(\varepsilon) \triangleq \{\mathbf{e} \,|\, \|\mathbf{e}\| \leq \varepsilon\}.$$

Applying the triangle and Cauchy–Schwarz inequalities along with the inequality $\|\mathbf{e}\| \leq \varepsilon$, we have that

$$|\mathbf{w}^H \mathbf{a} + \mathbf{w}^H \mathbf{e}| \geq |\mathbf{w}^H \mathbf{a}| - |\mathbf{w}^H \mathbf{e}| \geq |\mathbf{w}^H \mathbf{a}| - \varepsilon \|\mathbf{w}\|. \tag{23}$$

Moreover, it is easy to verify that

$$|\mathbf{w}^H \mathbf{a} + \mathbf{w}^H \mathbf{e}| = |\mathbf{w}^H \mathbf{a}| - \varepsilon \|\mathbf{w}\| \tag{24}$$

if ε is small enough (i.e., if $|\mathbf{w}^H \mathbf{a}| > \varepsilon \|\mathbf{w}\|$) and if

$$\mathbf{e} = -\frac{\mathbf{w}}{\|\mathbf{w}\|} \varepsilon \, e^{j\phi}$$

where

$$\phi = \text{angle} \left\{ \mathbf{w}^H \mathbf{a} \right\}.$$

Note that we require that $|\mathbf{w}^H \mathbf{a}| > \varepsilon \|\mathbf{w}\|$, as otherwise, the white noise gain of the robust beamformer may be insufficient [18].

Then, combining (23) and (24), we conclude that

$$\min_{\mathbf{c} \in \mathcal{A}(\varepsilon)} |\mathbf{w}^H \mathbf{c}| = |\mathbf{w}^H \mathbf{a}| - \varepsilon \|\mathbf{w}\|$$

and therefore, the semi-infinite nonconvex quadratically constrained problem (22) can be written as the following quadratic minimization problem with a *single* nonlinear constraint:

$$\min_{\mathbf{w}} \mathbf{w}^H \hat{R} \mathbf{w} \qquad \text{subject to} \qquad |\mathbf{w}^H \mathbf{a}| - \varepsilon \|\mathbf{w}\| \geq 1. \tag{25}$$

The nonlinear constraint in (25) is still nonconvex due to the absolute value operation on the left-hand side. An important observation is that the cost function in (25) is *unchanged* when $\mathbf{w}$ undergoes an arbitrary phase rotation. Therefore, if $\mathbf{w}_0$ is an optimal solution to (25), we can always rotate, without affecting the objective function value, the phase of $\mathbf{w}_0$ so that $\mathbf{w}^H \mathbf{a}$ is real. Thus, we can, without any loss of generality, choose $\mathbf{w}$ such that

$$\text{Re} \left\{ \mathbf{w}^H \mathbf{a} \right\} \geq 0 \tag{26}$$

$$\text{Im} \left\{ \mathbf{w}^H \mathbf{a} \right\} = 0. \tag{27}$$

Using this observation and employing (26) and (27) as additional constraints, the constraint in (25) can be written as

$$\boldsymbol{w}^H \boldsymbol{a} \geq \varepsilon \|\boldsymbol{w}\| + 1. \tag{28}$$

From (28) along with (27), it follows that $\mathrm{Re}\left\{\boldsymbol{w}^H \boldsymbol{a}\right\} \geq 0$. Since the constraint (26) is taken into account by (27) and (28), there is no need to add this constraint to the minimization problem (25). Therefore, this problem can be rewritten as

$$\min_{\boldsymbol{w}} \boldsymbol{w}^H \hat{\boldsymbol{R}} \boldsymbol{w} \quad \text{subject to } \boldsymbol{w}^H \boldsymbol{a} \geq \varepsilon \|\boldsymbol{w}\| + 1$$
$$\mathrm{Im}\left\{\boldsymbol{w}^H \boldsymbol{a}\right\} = 0. \tag{29}$$

Note that the problem (29) has much simpler formulation than (21) and is *convex*.

B. Relationship to the LSMI Beamformer

To clarify the problem (29) more, note that the constraint in (22) is equivalent to

$$\min_{\boldsymbol{c} \in \mathcal{A}(\varepsilon)} |\boldsymbol{w}^H \boldsymbol{c}| = 1 \tag{30}$$

or, in other words, (29) corresponds to maximization of the worst-case output SINR. The equivalence of the equality constraint (30) and the inequality constraint in (22) can be easily proved by contradiction as follows. If they are not equivalent to each other, then the minimum of the objective function in (22) is achieved when $\kappa \triangleq \min_{\boldsymbol{c} \in \mathcal{A}(\varepsilon)} |\boldsymbol{w}^H \boldsymbol{c}| > 1$. However, replacing $\boldsymbol{w}$ with $\boldsymbol{w}/\sqrt{\kappa}$, we can decrease the objective function $\boldsymbol{w}^H \hat{\boldsymbol{R}} \boldsymbol{w}$ by the factor of $\kappa > 1$, whereas the constraint in (22) will be still satisfied. This contradicts the original statement that the objective function is minimized when $\kappa > 1$. Therefore, the minimum of the objective function is achieved at $\kappa = 1$, and this proves that the inequality constraint in (29) is equivalent to the equality constraint $\boldsymbol{w}^H \boldsymbol{a} = \varepsilon \|\boldsymbol{w}\| + 1$. Therefore, $\boldsymbol{w}^H \boldsymbol{a}$ is real-valued and positive, and the constraint $\mathrm{Im}\left\{\boldsymbol{w}^H \boldsymbol{a}\right\} = 0$ can be ignored. Using these facts, we can rewrite the problem (29) as

$$\min_{\boldsymbol{w}} \boldsymbol{w}^H \hat{\boldsymbol{R}} \boldsymbol{w} \quad \text{subject to} \quad |\boldsymbol{w}^H \boldsymbol{a} - 1|^2 = \varepsilon^2 \boldsymbol{w}^H \boldsymbol{w}. \tag{31}$$

The solution to (31) can be found by minimizing the function

$$H(\boldsymbol{w}, \lambda) = \boldsymbol{w}^H \hat{\boldsymbol{R}} \boldsymbol{w}$$
$$+ \lambda(\varepsilon^2 \boldsymbol{w}^H \boldsymbol{w} - \boldsymbol{w}^H \boldsymbol{a} \boldsymbol{a}^H \boldsymbol{w} + \boldsymbol{w}^H \boldsymbol{a} + \boldsymbol{a}^H \boldsymbol{w} - 1)$$

where λ is a Lagrange multiplier. Taking the gradient of $H(\boldsymbol{w}, \lambda)$ and equating it to zero gives

$$\boldsymbol{w} = -\lambda \left(\hat{\boldsymbol{R}} + \lambda \varepsilon^2 \boldsymbol{I} - \lambda \boldsymbol{a} \boldsymbol{a}^H\right)^{-1} \boldsymbol{a}.$$

Applying the matrix inversion lemma to the latter equation, we obtain

$$\boldsymbol{w} = \frac{\lambda}{\lambda \boldsymbol{a}^H (\hat{\boldsymbol{R}} + \lambda \varepsilon^2 \boldsymbol{I})^{-1} \boldsymbol{a} - 1} (\hat{\boldsymbol{R}} + \lambda \varepsilon^2 \boldsymbol{I})^{-1} \boldsymbol{a} \tag{32}$$

which shows that the proposed robust beamformer belongs to the class of diagonal loading techniques.

Note, however, that it is not easy to use (32) directly for computing the optimal weight vector because it is not clear how to obtain the Lagrange multiplier λ in a closed form [26]. Therefore, to solve (29), an efficient SOC programming-based approach is developed in the next section.

C. SOC Implementation

The next step involves developing a SOC formulation of (29). Note that although we have shown in the previous section that the inequality constraint in (29) can be replaced by equality, we will use this constraint in its original inequality form, which is suitable for the SOC implementation.

First of all, we convert the quadratic objective function of (29) to a linear one. Let

$$\hat{\boldsymbol{R}} = \boldsymbol{U}^H \boldsymbol{U} \tag{33}$$

be the Cholesky factorization of $\hat{\boldsymbol{R}}$. Using (33), we can convert the objective function of (29) into

$$\boldsymbol{w}^H \hat{\boldsymbol{R}} \boldsymbol{w} = \|\boldsymbol{U} \boldsymbol{w}\|^2. \tag{34}$$

Apparently, minimizing $\|\boldsymbol{U} \boldsymbol{w}\|$ is equivalent to minimizing (34). Hence, introducing a new scalar non-negative variable τ and a new constraint $\|\boldsymbol{U} \boldsymbol{w}\| \leq \tau$, we can convert (29) into the following problem:

$$\min_{\tau, \boldsymbol{w}} \tau \quad \text{subject to } \|\boldsymbol{U} \boldsymbol{w}\| \leq \tau$$
$$\varepsilon \|\boldsymbol{w}\| \leq \boldsymbol{w}^H \boldsymbol{a} - 1$$
$$\mathrm{Im}\left\{\boldsymbol{w}^H \boldsymbol{a}\right\} = 0. \tag{35}$$

To facilitate the solution of (35), we need to convert it to a real-valued form. Introducing

$$\breve{\boldsymbol{w}} \triangleq \left[\mathrm{Re}\{\boldsymbol{w}\}^T, \mathrm{Im}\{\boldsymbol{w}\}^T\right]^T$$
$$\breve{\boldsymbol{a}} \triangleq \left[\mathrm{Re}\{\boldsymbol{a}\}^T, \mathrm{Im}\{\boldsymbol{a}\}^T\right]^T$$
$$\bar{\boldsymbol{a}} \triangleq \left[\mathrm{Im}\{\boldsymbol{a}\}^T, -\mathrm{Re}\{\boldsymbol{a}\}^T\right]^T$$
$$\breve{\boldsymbol{U}} \triangleq \begin{bmatrix} \mathrm{Re}\{\boldsymbol{U}\} & -\mathrm{Im}\{\boldsymbol{U}\} \\ \mathrm{Im}\{\boldsymbol{U}\} & \mathrm{Re}\{\boldsymbol{U}\} \end{bmatrix}$$

we rewrite (35) in terms of real-valued vectors and matrices as

$$\min_{\tau, \breve{\boldsymbol{w}}} \tau \quad \text{subject to } \|\breve{\boldsymbol{U}} \breve{\boldsymbol{w}}\| \leq \tau$$
$$\varepsilon \|\breve{\boldsymbol{w}}\| \leq \breve{\boldsymbol{w}}^T \breve{\boldsymbol{a}} - 1$$
$$\breve{\boldsymbol{w}}^T \bar{\boldsymbol{a}} = 0. \tag{36}$$

Let us define

$$\boldsymbol{d} \triangleq [1, \boldsymbol{0}^T]^T \in \mathcal{R}^{(2M+1) \times 1}$$
$$\boldsymbol{y} \triangleq [\tau, \breve{\boldsymbol{w}}^T]^T \in \mathcal{R}^{(2M+1) \times 1}$$
$$\boldsymbol{f} \triangleq [\boldsymbol{0}^T, -1, \boldsymbol{0}^T]^T \in \mathcal{R}^{(4M+3) \times 1}$$
$$\boldsymbol{F}^T \triangleq \begin{bmatrix} 1 & \boldsymbol{0}^T \\ \boldsymbol{0} & \breve{\boldsymbol{U}} \\ \boldsymbol{0} & \breve{\boldsymbol{a}}^T \\ \boldsymbol{0} & \varepsilon \boldsymbol{I} \\ \boldsymbol{0} & \bar{\boldsymbol{a}}^T \end{bmatrix} \in \mathcal{R}^{(4M+3) \times (2M+1)}$$

where $\boldsymbol{0}$ is the vector of zeros of a conformable dimension. With these notations, (36) can be further transformed to the following

canonical *dual* form[7] of the SOC programming problem (which is equivalent to (8) in [29]):

$$\min_{\boldsymbol{y}} \boldsymbol{d}^T \boldsymbol{y} \quad \text{subject to}$$

$$\boldsymbol{f} + \boldsymbol{F}^T \boldsymbol{y} \in \text{SOC}_1^{2M+1} \times \text{SOC}_2^{2M+1} \times \{0\} \quad (37)$$

where $\boldsymbol{y}$ is the vector of variables, SOC_i^{2M+1} is the second-order cone of the dimension $2M + 1$, which corresponds to the ith inequality constraint in (36) ($i = 1, 2$), and $\{0\}$ is the so-called zero cone that determines the hyperplane due to the equality constraint $\breve{\boldsymbol{w}}^T \bar{\boldsymbol{a}} = 0$. More specifically

$$\text{SOC}_i^{2M+1} \triangleq \left\{ \tilde{\boldsymbol{p}}_i \in \mathcal{R}^{2M+1} \mid p_i \geq \|\bar{\boldsymbol{p}}_i\| \right\}, \quad i = 1, 2$$

$$\{0\} \triangleq \{p_{4M+3} \in \mathcal{R} \mid p_{4M+3} = 0\}$$

where

$$\boldsymbol{p} \triangleq \left[\tilde{\boldsymbol{p}}_1^T, \tilde{\boldsymbol{p}}_2^T, p_{4M+3} \right]^T$$
$$= \left[\tau, \breve{\boldsymbol{w}}^T \breve{\boldsymbol{U}}^T, \breve{\boldsymbol{w}}^T \breve{\boldsymbol{a}} - 1, \varepsilon \breve{\boldsymbol{w}}^T, \breve{\boldsymbol{w}}^T \bar{\boldsymbol{a}} \right]^T$$
$$= \boldsymbol{f} - \boldsymbol{F}^T \boldsymbol{y}$$
$$\tilde{\boldsymbol{p}}_1 \triangleq \left[p_1, \bar{\boldsymbol{p}}_1^T \right]^T$$
$$= \left[\tau, \breve{\boldsymbol{w}}^T \breve{\boldsymbol{U}}^T \right]^T$$
$$\tilde{\boldsymbol{p}}_2 \triangleq \left[p_2, \bar{\boldsymbol{p}}_2^T \right]^T$$
$$= \left[\breve{\boldsymbol{w}}^T \breve{\boldsymbol{a}} - 1, \varepsilon \breve{\boldsymbol{w}}^T \right]^T$$
$$p_{4M+3} \triangleq \breve{\boldsymbol{w}}^T \bar{\boldsymbol{a}}.$$

Note that after solving the optimization problem (37), the only parameters of interest in the vector of variables $\boldsymbol{y}$ are given by its subvector $\tilde{\boldsymbol{w}}$. The resulting weight vector of our robust adaptive beamformer is given by

$$\boldsymbol{w}_{\text{rob}} = [\tilde{w}_1, \ldots, \tilde{w}_M]^T + j[\tilde{w}_{M+1}, \ldots, \tilde{w}_{2M}]^T. \quad (38)$$

In summary, we converted the robust beamforming problem (21) to the canonical SOC problem (37). Note that although these problems are mathematically equivalent, the original problem (21) is computationally intractable, whereas the SOC problem (37) can be easily solved using standard and highly efficient interior point method software tools, e.g., [29]. For example, using the primal-dual potential reduction method [27], the complexity of our beamformer is $O(M^3)$ per iteration [28], and the algorithm converges typically in less than ten iterations (a well-known and accepted fact in the optimization community). Therefore, the overall complexity of our beamformer is $O(M^3)$. This is the same order of complexity as that of the SMI algorithm. However, the SMI algorithm has a computational advantage in the *on-line mode*, where the RLS algorithm can be used to update the SMI beamformer weights with the computational complexity $O(M^2)$ per updating step. The weight vector of our beamformer cannot be easily updated but has to be recomputed in each step.

---

[7]Both dual and primal forms of SOC programming problems can be alternatively used when applying the SeDuMi software of [29].
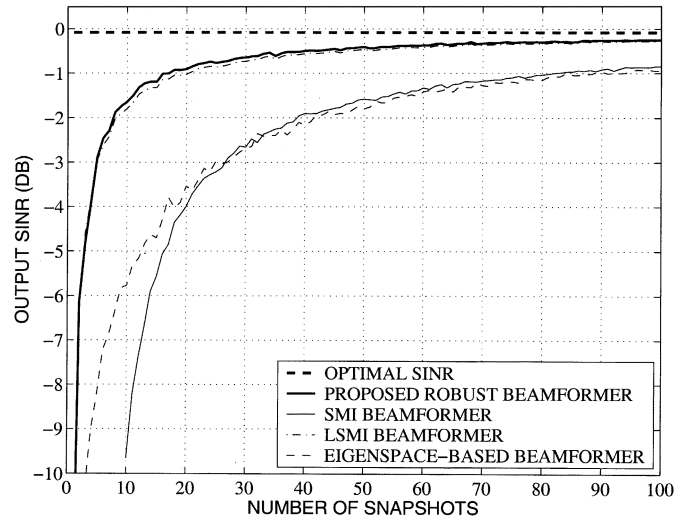

Fig. 1. Output SINR versus training sample size N; first example.

IV. SIMULATIONS

In our simulations, we assume a uniform linear array with $M = 10$ omnidirectional sensors spaced half a wavelength apart. For each scenario, 200 simulation runs are used to obtain each simulated point. In all examples, we assume two interfering sources with plane wavefronts and the directions of arrival (DOAs) 30° and 50°, respectively. In all simulations, the interference-to-noise ratio (INR) in a single sensor is equal to 30 dB, and the signal is always present in the training data cell. Four methods are compared in terms of the mean output SINR: the proposed robust beamformer (38), the SMI beamformer (8), the LSMI beamformer (14) with *ad hoc* choice of the diagonal load,[8] and the eigenspace-based beamformer (17). The optimal SINR (12) is also shown in all figures. The SeDuMi convex optimization MATLAB toolbox [29] has been used to compute the weight vector of our robust beamformer that employs the constant $\varepsilon = 3$ throughout the simulations (except one simulation in the first example, where ε is varied; see Fig. 3), assuming that the nominal steering vector is normalized so that $\boldsymbol{a}^H \boldsymbol{a} = M (= 10)$. The diagonal loading factor $\xi = 10\sigma^2$ is taken in the LSMI beamformer. Furthermore, diagonal loading with the same parameter is applied to our robust technique as well but only in the case when the sample covariance matrix is low rank (i.e., in the case when $N < M$).

A. Example 1: Exactly Known Signal Steering Vector

In this example, we simulate a scenario where the actual spatial signature of the signal is known exactly. Note that even in this ideal case, the presence of the signal of interest in the training data cell may substantially reduce the convergence rates of adaptive beamforming algorithms as compared with the signal-free training data case [6].

In this example, the plane-wave signal is assumed to impinge on the array from $\theta_s = 3°$. Fig. 1 compares four aforementioned methods in terms of the mean output array SINR (11) versus the number of training snapshots N for the fixed single-sensor

---

[8]This beamformer is hereafter referred to as the *ad hoc* LSMI technique.
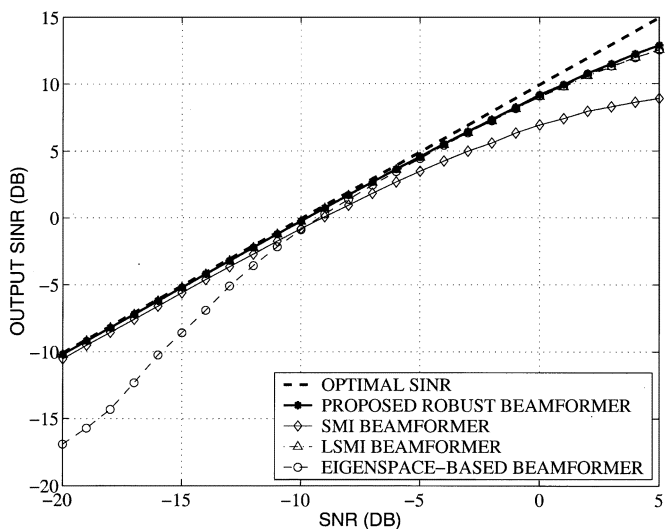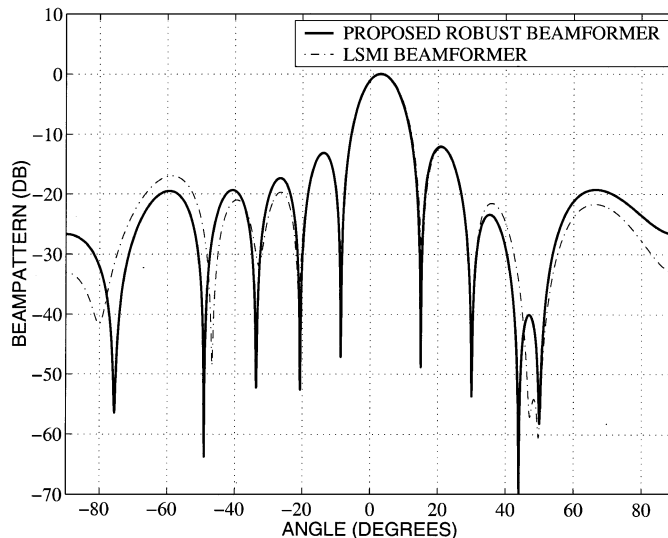
Fig. 2. Output SINR versus SNR; first example.

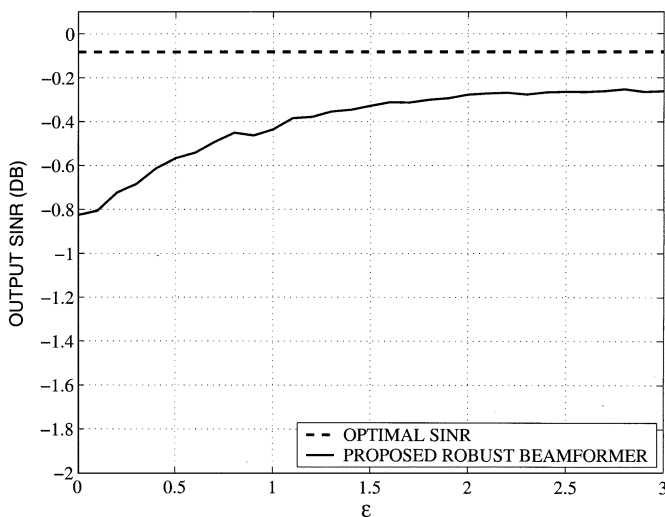Fig. 4. Beampatterns of the proposed and *ad hoc* LSMI beamformers; first example.

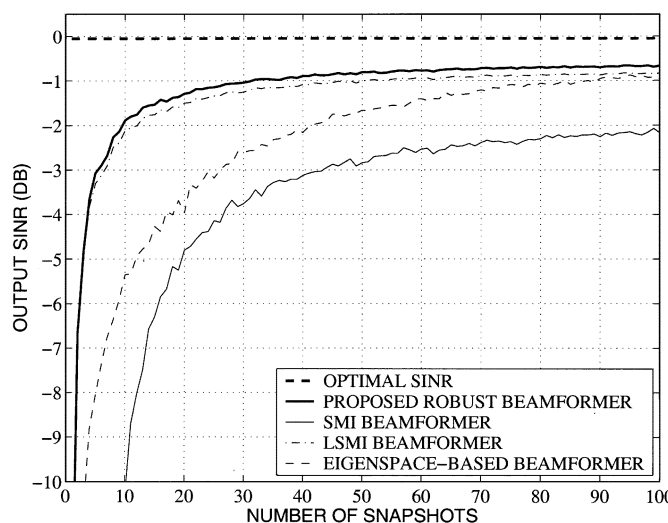Fig. 3. Output SINR versus ε; first example.

Fig. 5. Output SINR versus training sample size N; second example.

SNR $= -10$ dB. Fig. 2 displays the performance of these techniques versus the SNR for the fixed training data size $N = 30$. Fig. 3 shows the performance of the methods tested versus ε for $N = 100$ and SNR$= -10$ dB. Additionally, the beampatterns of our beamformer and the *ad hoc* LSMI algorithm are compared in Fig. 4 for $N = 40$ and SNR$= -10$ dB.

B. Example 2: Signal Look Direction Mismatch

In the second example, a scenario with the signal look direction mismatch is considered. We assume that both the presumed and actual signal spatial signatures are plane waves impinging from the DOAs 3 and 5°, respectively. This corresponds to a 2° mismatch in the signal look direction.

Fig. 5 shows the performance of the methods tested versus the number of training snapshots N for the fixed SNR$= -10$ dB. The performance of these algorithms versus the SNR for the fixed training data size $N = 30$ is shown in Fig. 6.
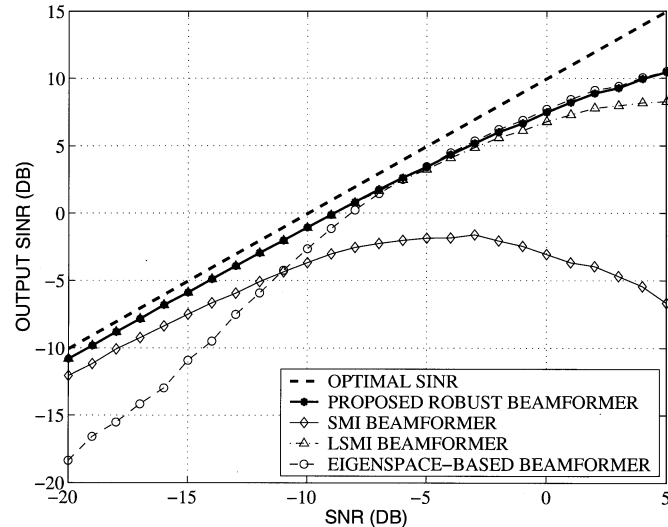
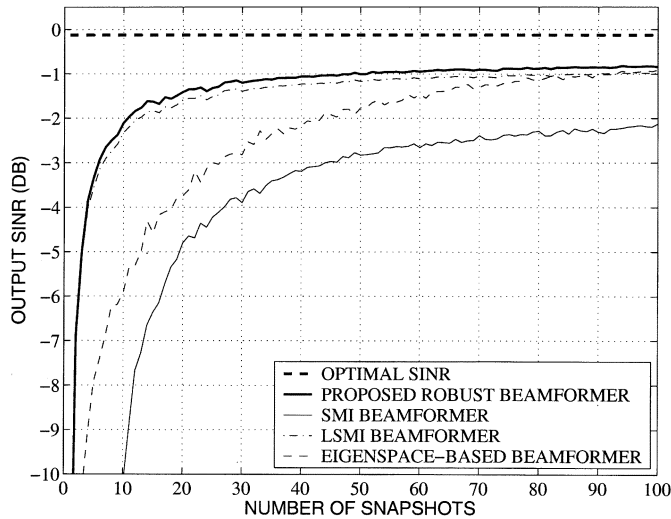Fig. 6. Output SINR versus SNR; second example.

Fig. 7.   Output SINR versus training sample size N; third example.

Fig. 8.   Output SINR versus SNR; third example.

C. Example 3: Signal Spatial Signature Mismatch Due to Coherent Local Scattering

Our third example corresponds to the scenario where the spatial signature of the desired signal is distorted by local scattering effects. In this example, the presumed signal spatial signature is a plane wave impinging on the array from $3°$, whereas the actual spatial signature is formed by five signal paths and is given by

$$\tilde{\boldsymbol{a}} = \boldsymbol{a} + \sum_{i=1}^{4} e^{j\psi_i} \boldsymbol{b}(\theta_i) \tag{39}$$

where $\boldsymbol{a}$ corresponds to the direct path, whereas $\boldsymbol{b}(\theta_i)$ ($i = 1, 2, 3, 4$) correspond to the coherently scattered paths. We model the ith path $\boldsymbol{b}(\theta_i)$ as a a plane wave impinging on the array from the direction θ_i. The parameters θ_i, $i = 1, 2, 3, 4$ are independently drawn in each simulation run from a uniform random generator with mean $= 3°$ and standard deviation $= 2°$. The parameters ψ_i, $i = 1, 2, 3, 4$ represent path phases that are independently and uniformly drawn from the interval $[0, 2\pi]$ in each simulation run. Note that θ_i and ψ_i ($i = 1, 2, 3, 4$) change from run to run while remaining frozen from snapshot to snapshot. This case corresponds to the so-called coherent scattering [14].

Fig. 7 displays the performance of the methods tested versus the number of training snapshots N for the fixed single-sensor SNR$= -10$ dB. Note that the SNR in this example is defined by taking into account all signal paths.

The performance of the same methods versus the SNR for the fixed training data size $N = 30$ is displayed in Fig. 8.

D. Example 4: Signal Spatial Signature Mismatch Due to Incoherent Local Scattering

In this example, we assume incoherent local scattering of the desired signal. The signal is assumed to have a time-varying spatial signature that is different for each data snapshot and is modeled as

$$\tilde{\boldsymbol{a}}(k) = s_0(k)\boldsymbol{a} + \sum_{i=1}^{4} s_i(k)\boldsymbol{b}(\theta_i)$$

where $s_i(k)$ are i.i.d. zero-mean complex Gaussian random variables independently drawn from a random generator. As in the previous example, the DOAs θ_i, $i = 1, 2, 3, 4$ are independently drawn in each simulation run from a uniform random generator with mean $= 3°$ and standard deviation $= 2°$. Note that the DOAs θ_i change from run to run while remaining fixed from snapshot to snapshot. At the same time, the random variables $s_i(k)$ change both from run to run and from snapshot to snapshot. This corresponds to the case of incoherent local scattering [15], where the signal covariance matrix $\boldsymbol{R}_s$ is no longer a rank-one matrix, and (11) for the output SINR should be rewritten in a more general form [17]

$$\text{SINR} = \frac{\boldsymbol{w}^H \boldsymbol{R}_s \boldsymbol{w}}{\boldsymbol{w}^H \boldsymbol{R}_{i+n} \boldsymbol{w}}. \tag{40}$$

The ratio (40) is maximized by [17]

$$\boldsymbol{w}_{\text{opt}} = \mathcal{P}\{\boldsymbol{R}_{i+n}^{-1} \boldsymbol{R}_s\} \tag{41}$$

where $\mathcal{P}\{\cdot\}$ is the operator that computes the principal eigenvector of a matrix. Note that solution (41) is of a little practical use because in most applications, the matrix $\boldsymbol{R}_s$ is unknown, and no reasonable estimate of it is available.

Fig. 9 displays the performance of the methods tested versus the number of training snapshots N with the fixed SNR $= -10$ dB. As in the previous example, the SNR is defined by taking into account all signal paths.

The performance of the same methods versus the SNR for the fixed training data size $N = 30$ is displayed in Fig. 10. We stress that the optimal SINR for Figs. 9 and 10 is computed as

$$\text{SINR}_{\text{opt}} = \frac{\boldsymbol{w}_{\text{opt}}^H \boldsymbol{R}_s \boldsymbol{w}_{\text{opt}}}{\boldsymbol{w}_{\text{opt}}^H \boldsymbol{R}_{i+n} \boldsymbol{w}_{\text{opt}}}$$

where $\boldsymbol{w}_{\text{opt}}$ is given by (41).

E. Example 5: Near–Far Signal Spatial Signature Mismatch

In the fifth example, we model the so-called near-far spatial signature mismatch of the desired signal. In this example, the
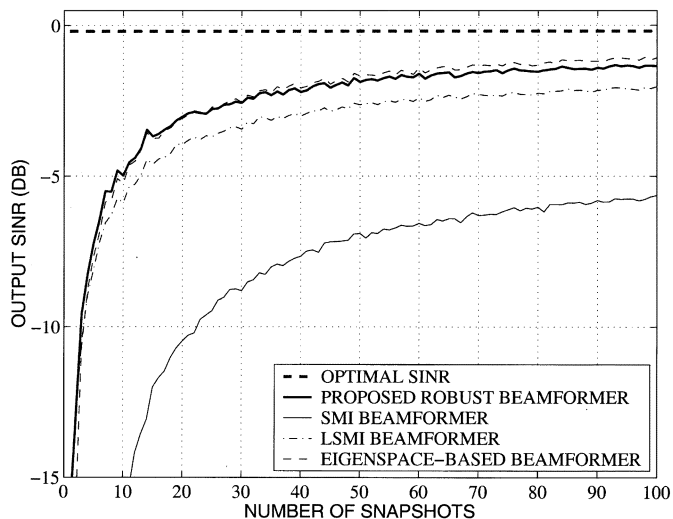
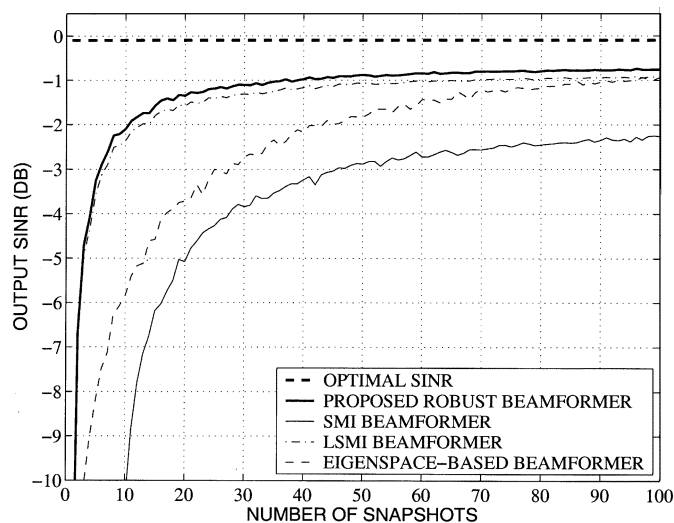Fig. 9.   Output SINR versus training sample size N; fourth example.

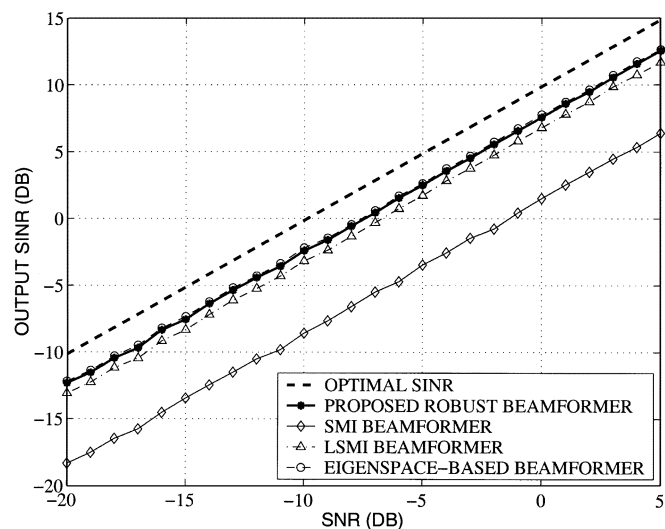Fig. 11.   Output SINR versus training sample size N; fifth example.

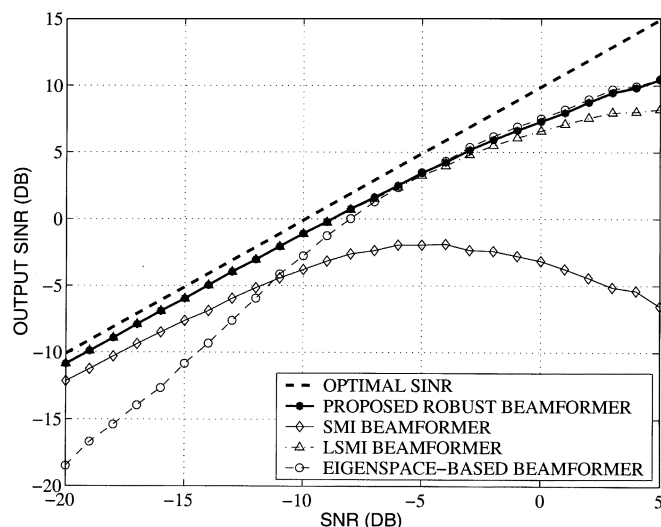Fig. 10.   Output SINR versus SNR; fourth example.

Fig. 12.   Output SINR versus SNR; fifth example.

presumed spatial signature of the signal is a plane wave impinging on the array from the normal direction 0°, whereas the actual spatial signature corresponds to the source located in the near field of the antenna at a distance $D^2/\lambda = (M-1)^2\lambda/4$ from the geometrical center of the array, where $D = (M-1)\lambda/2$ is the length of array aperture.[9] The source is assumed to be located on the line which is drawn from this geometrical center point in the normal direction to the array aperture.

The performance of the methods tested versus the number of training snapshots N for the fixed SNR= -10 dB is shown in Fig. 11. Fig. 12 shows the performance of these techniques versus the SNR for the fixed training data size $N = 30$.

F. Example 6: Signal Spatial Signature Mismatch Due to Wavefront Distortion

In our last example, we simulate the situation when the signal spatial signature is distorted by wave propagation effects in an inhomogeneous medium. We assume independent-increment

[9]Far field condition requires that the distance between the source and antenna remains much larger than D^2/λ [38].

phase distortions of the desired signal wavefront [11], [39]. In each simulation run, each of these phase distortions (which remains fixed for all snapshots) is independently drawn from a Gaussian random generator with variance equal to 0.04.

Fig. 13 shows the performance of the methods tested versus N for the fixed SNR= -10 dB. The performance of these techniques versus the SNR for the fixed training data size $N = 30$ is shown in Fig. 14.

G. Discussion

Our simulation figures clearly demonstrate that in all examples, the proposed robust beamformer consistently enjoys the best performance among the methods tested. Indeed, our new method outperforms the SMI, *ad hoc* LSMI, and eigenspace-based beamformers, achieving a performance that is consistently close to the optimal SINR for all values of SNR. The *ad hoc* LSMI algorithm is another well-performing method as its performance is comparable with that of our robust beamformer in a part of the examples tested. This can be explained by the fact discovered in Section III that our beamformer] be-
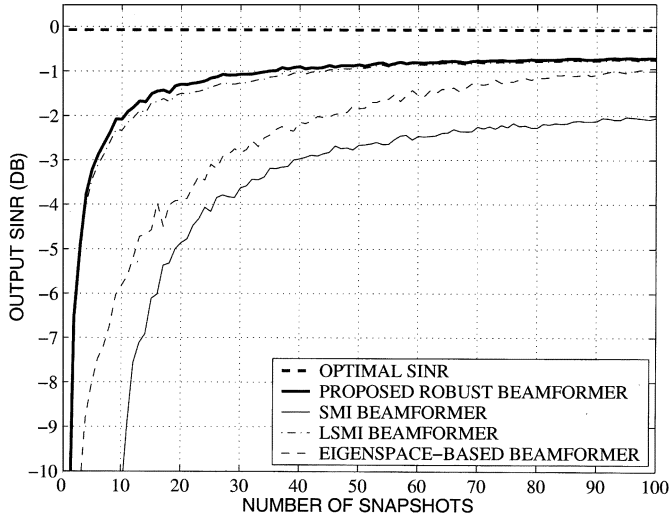
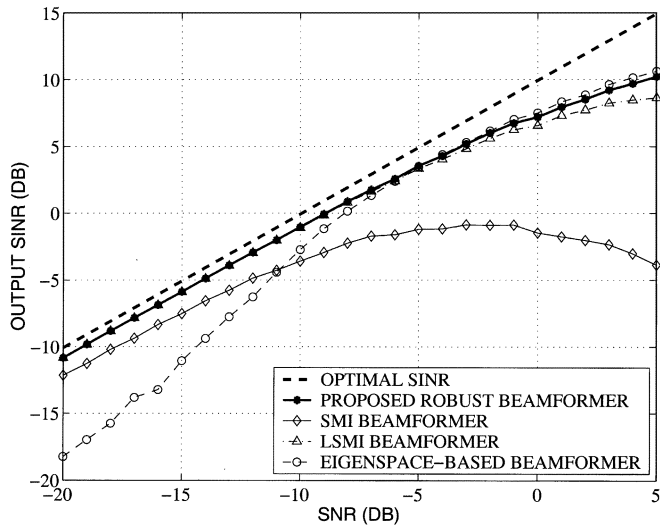Fig. 13.   Output SINR versus training sample size N; sixth example.

Fig. 14.   Output SINR versus SNR; sixth example.

longs to the class of diagonal loading techniques. However, our algorithm performs better than the *ad hoc* LSMI method in the fourth example at all SNRs (Figs. 9 and 10) and in the second, third, fifth, and sixth examples at high SNRs (Figs. 6, 8, 12 and 14). Note that in these examples, the aforementioned performance gains of our beamformer as compared with the *ad hoc* LSMI method can achieve 2 dB. Clearly, this improvement in performance is due to a more proper choice of the diagonal loading factor in our beamformer as compared with the *ad hoc* LSMI beamformer.

The performance of the SMI and eigenspace-based beamformers is much worse than that of the proposed beamformer and the *ad hoc* LSMI beamformer either at high SNRs (as in the case of SMI beamformer: Figs. 2, 6, 8, 12, and 14) or at low SNRs (as in the case of eigenspace-based beamformer, the same figures). Moreover, in the fourth example, the SMI algorithm shows poor performance at all values of the SNR (see Fig. 10). Note that the performance breakdown of the eigenspace-based

beamformer at low SNRs is caused by the subspace swap effect [31], [32], whereas the aforementioned performance losses of the SMI algorithm at high SNRs are due to the fact that increasing the amount of the signal component in the training data is known to lead to a substantial degradation[10] of the output SINR of SMI-type beamformers [6]. Furthermore, from Figs. 1, 5, 7, 9, 11, and 13, it follows that the proposed algorithm enjoys much faster convergence rate than the SMI and eigenspace-based algorithms. It is worth noting that even in the situation without any steering vector mismatch (Example 1, Figs. 1 and 2), the proposed technique has substantially better performance and faster convergence rate than the SMI and eigenspace-based beamformers.

Fig. 3 demonstrates that the proposed beamformer is insensitive to the choice of the parameter ε, whereas Fig. 4 shows that the beampatterns of the proposed beamformer and the LSMI beamformer are very similar to each other. This can be explained by the above-mentioned fact that the proposed beamformer is equivalent to the LSMI beamformer whose diagonal loading factor is optimally matched to the known level of the steering vector distortion.

V. CONCLUSIONS

A new adaptive beamformer with an improved robustness against an arbitrary unknown signal steering vector mismatch has been proposed. Our technique optimizes the worst-case performance by minimizing the output interference-plus-noise power while maintaining a distortionless response for the worst-case (mismatched) signal steering vector. A convex formulation for such a robust adaptive beamforming problem is derived using second-order cone programming. It is shown that the proposed beamformer can be interpreted as a diagonal loading approach whose optimal diagonal loading factor is precisely computed based on the known level of uncertainty in the signal steering vector. Computer simulations with several frequently encountered types of signal steering vector mismatch show better performance of the proposed beamformer as compared with several popular robust adaptive beamforming algorithms.

In addition to the offered performance improvements relative to existing methods, the proposed beamformer enjoys simple implementation. The order of computational complexity of this algorithm is comparable with that of the SMI technique. It can be efficiently implemented using currently available convex optimization software toolboxes based on interior point algorithms.

---

[10]This degradation occurs because the signal component "contaminates" the training observations (which in the ideal case must contain the interference and noise components only).

REFERENCES

[1] I. S. Reed, J. D. Mallett, and L. E. Brennan, "Rapid convergence rate in adaptive arrays," *IEEE Trans. Aerosp. Electron. Syst.*, vol. AES–10, pp. 853–863, Nov. 1974.

[2] L. J. Griffiths and C. W. Jim, "An alternative approach to linearly constrained adaptive beamforming," *IEEE Trans. Antennas Propagat.*, vol. AP–30, pp. 27–34, Jan. 1982.

[3] E. K. Hung and R. M. Turner, "A fast beamforming algorithm for large arrays," *IEEE Trans. Aerosp. Electron. Syst.*, vol. AES-19, pp. 598–607, July 1983.

[4] B. D. Carlson, "Covariance matrix estimation errors and diagonal loading in adaptive arrays," *IEEE Trans. Aerosp. Electron. Syst.*, vol. 24, pp. 397–401, July 1988.

[5] R. A. Monzingo and T. W. Miller, *Introduction to Adaptive Arrays*. New York: Wiley, 1980.

[6] D. D. Feldman and L. J. Griffiths, "A projection approach to robust adaptive beamforming," *IEEE Trans. Signal Processing*, vol. 42, pp. 867–876, Apr. 1994.

[7] L. C. Godara, "The effect of phase-shift errors on the performance of an antenna-array beamformer," *IEEE J. Ocean. Eng.*, vol. OE-10, pp. 278–284, July 1985.

[8] J. W. Kim and C. K. Un, "An adaptive array robust to beam pointing error," *IEEE Trans. Signal Processing*, vol. 40, pp. 1582–1584, June 1992.

[9] N. K. Jablon, "Adaptive beamforming with the generalized sidelobe canceller in the presence of array imperfections," *IEEE Trans. Antennas Propagat.*, vol. AP-34, pp. 996–1012, Aug. 1986.

[10] A. B. Gershman, V. I. Turchin, and V. A. Zverev, "Experimental results of localization of moving underwater signal by adaptive beamforming," *IEEE Trans. Signal Processing*, vol. 43, pp. 2249–2257, Oct. 1995.

[11] J. Ringelstein, A. B. Gershman, and J. F. Böhme, "Direction finding in random inhomogeneous media in the presence of multiplicative noise," *IEEE Signal Processing Lett.*, vol. 7, pp. 269–272, Oct. 2000.

[12] Y. J. Hong, C. C. Yeh, and D. R. Ucci, "The effect of a finite-distance signal source on a far-field steering Applebaum array—Two dimensional array case," *IEEE Trans. Antennas Propagat.*, vol. 36, pp. 468–475, Apr. 1988.

[13] K. I. Pedersen, P. E. Mogensen, and B. H. Fleury, "A stochastic model of the temporal and azimuthal dispersion seen at the base station in outdoor propagation environments," *IEEE Trans. Veh. Technol.*, vol. 49, pp. 437–447, Mar. 2000.

[14] J. Goldberg and H. Messer, "Inherent limitations in the localization of a coherently scattered source," *IEEE Trans. Signal Processing*, vol. 46, pp. 3441–3444, Dec. 1998.

[15] O. Besson and P. Stoica, "Decoupled estimation of DOA and angular spread for a spatially distributed source," *IEEE Trans. Signal Processing*, vol. 48, pp. 1872–1882, July 2000.

[16] D. Astely and B. Ottersten, "The effects of local scattering on direction of arrival estimation with MUSIC," *IEEE Trans. Signal Processing*, vol. 47, pp. 3220–3234, Dec. 1999.

[17] A. B. Gershman, "Robust adaptive beamforming in sensor arrays," *Int. J. Electron. Commun.*, vol. 53, pp. 305–314, Dec. 1999.

[18] H. Cox, R. M. Zeskind, and M. H. Owen, "Robust adaptive beamforming," *IEEE Trans. Acoust., Speech, Signal Processing*, vol. ASSP-35, pp. 1365–1376, Oct. 1987.

[19] K. L. Bell, Y. Ephraim, and H. L. Van Trees, "A Bayesian approach to robust adaptive beamforming," *IEEE Trans. Signal Processing*, vol. 48, pp. 386–398, Feb. 2000.

[20] M. H. Er and T. Cantoni, "An alternative formulation for an optimum beamformer with robustness capability," *Proc. Inst. Elect. Eng. Radar, Sonar, Navig.*, pp. 447–460, Oct. 1985.

[21] L. Chang and C. C. Yeh, "Performance of DMI and eigenspace-based beamformers," *IEEE Trans. Antennas Propagat.*, vol. 40, pp. 1336–1347, Nov. 1992.

[22] S. A. Vorobyov, A. B. Gershman, and Z.-Q. Luo, "An application of second-order cone programming to robust adaptive beamforming," in *Proc. 5th Int. Conf. Optim. Techn. Applicat.*, vol. 1, Hong Kong, Dec. 2001, pp. 308–315.

[23] ——, "Robust MVDR beamforming using worst-case performance optimization," in *Proc. 10th Workshop Adaptive Sensor Array Process.*. Lexington, MA, Mar. 2002.

[24] ——, "Robust adaptive beamforming using worst-case performance optimization via second-order cone programming," in *Proc. ICASSP*, Orlando, FL, May 2002, pp. 2901–2904.

[25] M. R. Garey and D. S. Johnson, *Computers and Intractability*. San Francisco, CA: W. H. Freeman, 1979.

[26] R. Lorenz and S. P. Boyd, "Robust minimum variance beamforming," *IEEE Trans. Signal Processing*, submitted for publication.

[27] Y. Nesterov and A. Nemirovsky, *Interior Point Polynomial Algorithms in Convex Programming*. Philadelphia, PA: SIAM, 1994.

[28] M. Lobo *et al.*, "Applications of second-order cone programming," *Linear Algebra Applicat.*, pp. 193–228, Nov. 1998.

[29] J. F. Sturm, "Using SeDuMi 1.02, a MATLAB toolbox for optimization over symmetric cones," *Optim. Meth. Softw.*, vol. 11–12, pp. 625–653, Aug. 1999.

[30] M. D. Zoltowski, "On the performance of the MVDR beamformer in the presence of correlated interference," *IEEE Trans. Acoust., Speech, Signal Processing*, vol. 36, pp. 945–947, June 1988.

[31] J. K. Thomas, L. L. Scharf, and D. W. Tufts, "The probability of a subspace swap in the SVD," *IEEE Trans. Signal Processing*, vol. 43, pp. 730–736, Mar. 1995.

[32] M. Hawkes, A. Nehorai, and P. Stoica, "Performance breakdown of subspace-based methods: Prediction and cure," in *Proc. ICASSP*, Salt Lake City, UT, May 2001, pp. 4005–4008.

[33] S. Cui, Z.-Q. Luo, and Z. Ding, "Robust blind multiuser detection against CDMA signature mismatch," in *Proc. ICASSP'01*, Salt Lake City, UT, May 2001, pp. 2297–2300.

[34] Z. Liu and Y. H. Hong, "Semi-infinite quadratic optimization method for the design of robust adaptive array processors," *Proc. Inst. Elect. Eng. Radar Sonar, Navig.*, vol. 137, pp. 177–183, June 1990.

[35] M. H. Er and A. Cantoni, "A new approach to the design of broadband element space antenna array processors," *IEEE J. Ocean. Eng.*, vol. OE-10, pp. 231–240, July 1985.

[36] B. D. Van Veen, "Minimum variance beamforming with soft response constraints," *IEEE Trans. Signal Processing*, vol. 39, pp. 1964–1972, Sept. 1991.

[37] H. Ye and R. D. DeGroat, "A generalized sidelobe canceller with soft constraints," *IEEE Trans. Signal Processing*, vol. 40, pp. 2112–2116, Aug. 1992.

[38] P. S. Naidu, *Sensor Array Signal Processing*. Boca Raton, FL: CRC, 2001.

[39] O. Besson, F. Vincent, P. Stoica, and A. B. Gershman, "Maximum likelihood estimation for array processing in multiplicative noise environments," *IEEE Trans. Signal Processing*, vol. 48, pp. 2506–2518, Sept. 2000.

Sergiy A. Vorobyov (M'02) was born in Ukraine in 1972. He received the M.S. and Ph.D. degrees in systems and control from Kharkiv National University of Radioelectronics (KNUR), Kharkiv, Ukraine, in 1994 and 1997, respectively.

From 1995 to 2000, he was with the Control and Systems Research Laboratory at KNUR, where he became a Senior Research Scientist in 1999. From 1999 to 2001, he was with the Brain Science Institute, RIKEN, Tokyo, Japan, as a Research Scientist. He is currently with the Department of Electrical and Computer Engineering, McMaster University, Hamilton, ON, Canada, as a Postdoctoral Fellow. In 1996 and 2002, respectively, he held short-time visiting appointments at the Institute of Applied Computer Science, Karlsruhe, Germany, and Gerhard-Mercator University, Duisburg, Germany. His research interests include control, statistical array signal processing, blind source separation, and robust adaptive beamforming.

Dr. Vorobyov was a recipient of the 1996–1998 Young Scientist Fellowship of the Ukrainian Cabinet of Ministers, the 1996 and 1997 Young Scientist Research Grants from the George Soros Foundation, and the 1999 DAAD Fellowship (Germany).

Alex B. Gershman (M'97–SM'98) received the Diploma (M.S.) and Ph.D. degrees in radiophysics from the Nizhny Novgorod State University, Nizhny Novgorod, Russia, in 1984 and 1990, respectively.

From 1984 to 1989, he was with the Radiotechnical and Radiophysical Institutes, Nizhny Novgorod. From 1989 to 1997, he was with the Institute of Applied Physics of Russian Academy of Science, Nizhny Novgorod, as a Senior Research Scientist. From the summer of 1994 until the beginning of 1995, he was a Visiting Research Fellow at the Swiss Federal Institute of Technology, Lausanne. From 1995 to 1997, he was Alexander von Humboldt Fellow at Ruhr University, Bochum, Germany. From 1997 to 1999, he was a Research Associate at the Department of Electrical Engineering, Ruhr University. In 1999, he joined the Department of Electrical and Computer Engineering, McMaster University, Hamilton, ON, Canada, as an Associate Professor, where he became a Full Professor in 2002. Currently, he also holds a Visiting Professorship at the Department of Communication Systems, Gerhard-Mercator University and Fraunhofer Institute for Microelectronic Circuits and Systems, Duisburg, Germany. His research interests are in the area of signal processing and include robust statistical signal and array processing, adaptive beamforming and smart antennas for mobile communications, signal parameter estimation and detection, spectral analysis, and signal processing applications to wireless communications, underwater acoustics, seismology, and radar.

Dr. Gershman was a recipient of the 1993 International Union of Radio Science (URSI) Young Scientist Award, the 1994 Outstanding Young Scientist Presidential Fellowship (Russia), the 1994 Swiss Academy of Engineering Science and Branco Weiss Fellowships (Switzerland), and the 1995–1996 Alexander von Humboldt Fellowship (Germany). He received the 2000 Premier's Research Excellence Award of Ontario and the 2001 Wolfgang Paul Award from the Alexander von Humboldt Foundation, Germany. He is also a recipient of the 2002 Young Explorers Prize from the Canadian Institute for Advanced Research (CIAR), which honors Canada's top 20 researchers aged 40 or under. Since 1999, he has been an Associate Editor of IEEE TRANSACTIONS ON SIGNAL PROCESSING and a Member of the Sensor Array and Multichannel (SAM) Signal Processing Technical Committee of the IEEE Signal Processing Society.

Zhi-Quan Luo (M'90) received the B.Sc. degree in applied mathematics in 1984 from Peking University, Beijing, China. Subsequently, he was selected by a joint committee of American Mathematical Society and the Society of Industrial and Applied Mathematics to pursue the Ph.D. degree in the United States. After a one-year intensive training in mathematics and English at the Nankai Institute of Mathematics, Tianjin, China, he was admitted to the Department of Electrical Engineering and Computer Science, Massachusetts Institute of Technology, Cambridge, where he received the Ph.D. degree in 1989.

Upon graduation, he joined the Department of Electrical and Computer Engineering, McMaster University, Hamilton, ON, Canada, where he is now the Department Head and holds a Canada Research Chair in Information Processing. His research interests lie in the union of large-scale optimization, data communication and signal processing, information theory, and coding.

Dr. Luo currently serves on the editorial boards for a number of international journals including the *SIAM Journal on Optimization* and the IEEE TRANSACTIONS ON SIGNAL PROCESSING. He is a recipient of the 2001 Award for the Best Paper at the International Conference on Optimization Techniques and Applications.